Journal of Chromatography, 577 (1992) 43–59
Biomedical Applications
Elsevier Science Publishers B.V., Amsterdam

CHROMBIO. 6312

pH titration curves of the desialylated human α_1-acid glycoprotein variants by combined isoelectrofocusing–electrophoresis: utilization in the development of a fractionation method for the protein variants by chromatography on immobilized metal affinity adsorbent

Françoise Hervé*, Jean-Claude Duché and Jérôme Barré

Laboratoire Hospitalo-Universitaire de Pharmacologie de Paris XII, Centre Hospitalier Intercommunal de Créteil, 40 Avenue de Verdun, 94010 Créteil Cedex (France)

Marie-Claude Millot

Laboratoire de Physicochimie des Biopolymères, Université Paris XII, Avenue du Général de Gaulle, 94010 Créteil Cedex (France)

Jean-Paul Tillement

Laboratoire Hospitalo-Universitaire de Pharmacologie de Paris XII, Centre Hospitalier Intercommunal de Créteil, 40 Avenue de Verdun, 94010 Créteil Cedex (France)

(First received November 15th, 1991; revised manuscript received January 22nd, 1992)

ABSTRACT

Using a two-dimensional isoelectrofocusing (IEF)–electrophoresis technique, the pH titration curves of the three main desialylated variants (F1, S and A) of human α_1-acid glycoprotein (AAG) were studied to assist in the development of a fractionation method for the AAG variants. For this purpose, different AAG samples, each corresponding to one of the three main phenotypes of the protein (F1S/A, F1/A and S/A), were first purified by chromatographic separation of individual human plasma samples on immobilized Cibacron Blue F3G-A. The purified AAG samples were then desialylated and their heterogeneity was checked by analytical IEF. The pH–mobility curves of the desialylated AAG samples were displayed in polyacrylamide gel slabs, under a constant set of experimental conditions, by carrying out electrophoresis of the protein samples perpendicularly to two stationary pH gradients: a large gradient (pH 3.5–9.5) and a narrow gradient (pH 5–8). The curves showed that all the desialylated variants of AAG exhibited small charge differences and moved closely together between about pH 3.5–5.5 and pH 7.5–9.5. However, the variants were found to show microheterogeneity in their total charge between about pH 5.5 and 7.5 due to the titrated ionizable groups involved along this pH zone. This microheterogeneity was assumed to be accounted for by the existence of differences between the titratable histidyl residues of the AAG variants. Consequently, the interactions of the variants with immobilized transition metal ions were studied at pH 7, using affinity chromatography on an iminodiacetate Sepharose–Cu(II) gel. It was found that the A variant was strongly bound by immobilized Cu(II) ions, whereas the F1 and S variants interacted non-specifically with the immobilized ligand. This finding allowed the development of a rapid and effective fractionation method for desialylated AAG into its A and F1 or S variants, depending on the AAG phenotype, by chromatography on an immobilized affinity Cu(II) adsorbent. The quantitative relationships between immobilized Cu(II) ions and desialylated AAG (the apparent association constant and gel protein-binding capacity) were also determined using a non-chromatographic equilibrium binding technique.

0378-4347/92/$05.00

INTRODUCTION

Human α_1-acid glycoprotein (AAG), or orosomucoid, is a plasma glycoprotein belonging to the group of "acute-phase reactants". Although its exact physiological function is still unknown, AAG has been identified in plasma as a transport protein for basic drugs, such as antidepressants, neuroleptics and β-blockers. This protein also seems to play a part in immunoregulation (for a review, see Kremer *et al.* [1]).

AAG is composed of a single polypeptide chain of 181 residues and has an estimated molecular mass of 44 kilodaltons. This glycoprotein has an unusually high carbohydrate content (up to 45%), consisting of a large number of sialyl residues (up to 11%) [2]. It has been well documented that AAG is very heterogeneous, consisting of sub-populations with different charges and lectin-binding behaviour [2,3].

The heterogeneity of human AAG has been extensively studied. After desialylation of this protein, three main variants are distinghuished by their electrophoretic migration in analytical isoelectrofocusing (IEF), as one "fast" and two "slow" bands [4], corresponding to the F1 and the S and A variants, respectively. These variants differ in the substitutions of several amino acids in the peptide chain [2,5]. This microheterogeneity is genetically determined and, depending on the relative concentrations of the variants in desialylated plasma, three main AAG phenotypes are observed in a general population: F1S/A, F1/A and S/A, the expected frequencies of which are 47.9, 35.1 and 16.4%, respectively [4].

Elucidation of this microheterogeneity, especially in the light of the possibility of functional (drug-binding) differences between the genetic variants of AAG is an interesting challenge and several studies have been carried out [6–9]. However, there have been several methodological difficulties. For example, the study of the binding properties to drugs of the individual genetic variants of human AAG requires the use of relatively large amounts of each variant because of the relatively low affinities to drugs generally described for human AAG (10^4–10^6 l/mol) [1]. However, the fractionation of AAG variants is generally performed using standard commercial proteins, which are mixtures of different AAG phenotypes. Two different methods, a preparative IEF method [7] and high-performance ion-exchange chromatography [10], have to be used successively for separating the three variants of desialylated AAG. In practice, we observed that the separation of the AAG variants is a relatively time-consuming procedure and above all that the recovery of each variant was low (less than 30–40% of each variant was recovered with both methods), thus making the study of the individual drug-binding properties of the variants a tedious task. Therefore, it appeared necessary to develop other fractionation methods for the AAG variants which would be simpler and more efficient than those used at present for separating AAG variants.

Therefore, we decided to study in parallel and under "native" conditions the pH titration curves of the desialylated variants of human AAG to assist us in the further development of other fractionation methods for the variants. For this purpose, small amounts of each of the three main AAG phenotype samples (F1S/A, F1/A and S/A) were purified in a first step after applying individual human plasma samples to Cibacron Blue F3G-A immobilized to Sephadex G-100 [10]. After purification, the AAG samples were desialylated and their respective pH titration curves were displayed in polyacrylamide gel slabs, under constant experimental conditions, by performing electrophoresis of the protein samples perpendicularly to different stationary pH gradients stabilized by a stack of focused carrier ampholytes [11]. The results obtained from this study led us to examine the binding of the variants to immobilized transition metal ions. Using a chromatographic method on an immobilized affinity Cu(II) adsorbent (IMAC) [12], the AAG variants were found to show important heterogeneity on binding to the immobilized ligand. This finding allowed us to develop an IMAC method for the fractionation of desialylated AAG samples into their F1S and A, or F1 and A, or S and A variants, depending on the pheno-

type of the sample used. The fractionation was then compared with the electrophoretic heterogeneity of the AAG samples as visualized by analytical IEF. In addition, the quantitative affinity relationships of immobilized Cu(II) ions with desialylated AAG were determined by using a non-chromatographic protocol, previously described by Hutchens *et al.* [13]. Our results are discussed in the light of the structural differences existing between the variants of human AAG.

EXPERIMENTAL

Materials

Human plasma samples containing AAG with the F1S/A, F1/A or S/A phenotype were obtained from healthy donors and frozen at −20°C until use.

Materials were obtained from the following sources. Human AAG (from Cohn fraction VI), essentially fatty acid free human serum albumin (from Cohn fraction V), *Clostridium perfringens* neuraminidase type X, Norite A charcoal, urea ultrapure and cupric chloride (ACS reagent) were from Sigma (St. Louis, MO, USA). Immobiline (p*K* 4.6 and 9.3), Ampholine carrier ampholytes (in the pH ranges 3.5–9.5 and 5–8, respectively), acrylamide, Gelbond polyacrylamide gel films, gradient gels PAA 4/30, low-molecular-mass marker protein kit, Sephadex G-100, chelating Sepharose Fast Flow (45–165 μm mean particle size, 22–30 μmol Cu^{2+} per ml gel) and columns PD-10 Sephadex G-25 M were purchased from Pharmacia LKB (Uppsala, Sweden). N,N′-Methylenebisacrylamide (bis), ammonium persulphate, N,N,N′,N′-tetramethylethylenediamine, Coomassie Brilliant Blue R 250, 2-mercaptoethanol and imidazole were obtained from Merck (Darmstadt, Germany), Cibacron Blue F3G-A was from Fluka (Buchs, Switzerland) and the YM 10 membrane filter and Centricon 10 microconcentrator were obtained from Amicon (Danvers, MA, USA). All other reagents were of grade A or analytical-reagent grade and were purchased from local suppliers.

Purification of individual AAG samples with different phenotypes on Cibacron Blue F3G-A immobilized to Sephadex G-100

The covalent coupling of Cibacron Blue F3G-A to Sephadex G-100 and the purification of the F1S/A, F1/A and S/A AAG samples from individual human plasma samples by a one-step chromatographic procedure on immobilized Cibacron Blue F3G-A were carried out as described previously [10]. The purity of each AAG preparation was checked by sodium dodecyl sulphate polyacrylamide gel electrophoresis (SDS-PAGE) [14], using a Pharmacia GE 2-4/LS vertical gel electrophoresis apparatus, and by immunoelectrophoresis [15] using a specific immunoserum to human plasma proteins (Behring, Marburg, Germany) and anti-human AAG rabbit immunoglobulins (Dakopatts, Glostrup, Denmark) as the antibodies.

Charcoal treatment and desialylation of AAG samples

Before use, the individually purified AAG samples and the commercial AAG sample were delipidated by charcoal treatment at pH 3.0 according to the method of Evenson and Deutsch [16] and then lyophilized. The proteins were then desialylated with neuraminidase [7], dialysed against deionized water and finally lyophilized.

Before analytical IEF, the individual human plasma samples used in the chromatographic procedure on immobilized Cibacron Blue were desialylated with neuraminidase as described by Eap *et al.* [4].

Spectrophotometry

Absorbance measurements or spectral scans were performed on a Beckman Model DU-7 single-beam recording spectrophotometer. The protein concentration of desialylated human AAG and of human serum albumin (HSA) were checked spectrophotometrically at 278 nm, using $A_1^{1\%}{}_{cm}$ values of 11.8 and 5.7 and assuming relative molecular mass (M_r) values of 39.2 and 65 kilodaltons for desialylated human AAG and HSA, respectively.

Isoelectrofocusing

An LKB 2117 Multiphor II electrophoresis apparatus was used for the IEF experiments.

Analytical IEF of the individual AAG samples, after their desialylation, and AAG phenotyping of the desialylated whole plasma were performed essentially as described by Eap and Baumann [17] in an immobilized pH 4.4–5.4 polyacrylamide gel gradient with 8 *M* urea and 2% (v/v) 2-mercaptoethanol. Detection of the variants was made by staining with Coomassie Brilliant Blue and by immunoblotting with two antibody steps [17], respectively. The relative proportion of each protein band in the gels was determined by scanning with an LKB 2202 Ultroscan laser densitometer.

The two-dimensional IEF–electrophoresis experiments were carried out according to LKB application Note 319 [18]. Polyacrylamide gel slabs (10.9 × 11.4 × 0.2 cm thick) containing 5% T, 3% C_{bis} and 2.4% Ampholine in the pH ranges 3.5–9.5 or 5–8 were cast with a narrow application trench in the middle (9 cm long × 1 mm wide × 1 mm deep) which could be filled with about 100 µl of sample. The pH gradient 3.5–9.5 was preformed (without sample) by the one-dimensional IEF of carrier ampholytes by delivering 10 W (with an LKB 2297 Macrodrive 5 constant-power supply) for 90 min at 4°C until steady-state conditions were reached (900 V, 11 mA), using cathodic and anodic paper strips soaked into 1 *M* NaOH and 1 *M* H_3PO_4, respectively. For performing the pH 5–8 gradient, 0.5 *M* NaOH and 0.5 *M* acetic acid were used as the catholyte and anolyte solutions, respectively, and steady-state conditions (1100 V, 9 mA) were reached by delivering 10 W (constant) for 75 min at 4°C. At this point, the anodic and cathodic regions were removed by slicing the gel on the inner side of the electrode filter-paper strips. The polyacrylamide gel was then turned around by 90° and new electrode paper strips, still containing the described anolyte and catholyte solutions, were applied for the second dimension. The application trench across the pH gradient was filled with the sample (depending on the AAG phenotype, 200–300 µg of desialylated AAG dissolved in 100 µl deionized water) and the two-dimensional electrophoresis of the protein was performed perpendicular to the pH gradient at 700 V for 25 min at 4°C to extend the titration curves over a large distance between the electrodes. At the end of the experiment the pH gradient was determined on the gel at 2–3 cm from the cathode or the anode, on a gel slice of 1 cm width, with a surface microelectrode (Ag/AgCl, 0.8 cm diameter, Lot 403-M8-S7/120, Ingold, Steinbach, Germany) combined with a digital Radiometer pH meter. Visualization of the protein titration curves was carried out by staining with Coomassie Brilliant Blue [18].

Experiments with immobilized Cu(II) ion to iminodiacetate (IDA) Sepharose

Equilibration of IDA Sepharose with metal adsorbent. The equilibration was performed at room temperature (20–23°C) according to the method of Hutchens *et al.* [13]. The chelating Sepharose was washed with several volumes of glass-distilled water over a Büchner recipient (porosity 4) and then poured into a glass column before loading with metal ions by equilibration with 0.2 *M* copper chloride in distilled water. Excess (unadsorbed) metal ions were removed by washing the IDA–Cu(II) gel with several volumes of pH 3.8, 0.1 *M* sodium acetate buffer, containing 0.5 *M* NaCl. Finally, the loaded IDA–Cu(II) gel was equilibrated with pH 7.0, 20 m*M* sodium phosphate buffer, containing 0.5 *M* NaCl (equilibration buffer E).

Immobilized metal ion-affinity chromatography. IDA Sepharose gel loaded with Cu(II) ions and equilibrated in buffer E (pH 7) was packed into glass columns (0.7 cm I.D.) to a final bed volume of 7.5 ml. Three types of AAG samples were used: a commercial AAG sample containing a mixture of the F1, S and A variants (total amount 5 mg), and individually purified AAG samples, consisting of either F1/A or S/A phenotype (total amount 1.5 mg). The AAG samples were all dissolved in 0.5 ml of column equilibration buffer E and separately applied to the columns at a linear flow-rate of 7.5 ml/h. Fractions (1.5 ml) were collected and their respective absor-

bances were measured spectrophotometrically at 280 nm. Next, several volumes of pH 7 buffer E were applied to remove the unbound variant(s); a second pH 7 elution buffer, consisting of 20 m*M* imidazole in buffer E, was applied to the columns to remove the bound variant(s). The columns were regenerated after each run by removing the metal with several volumes of 50 m*M* EDTA in buffer E. The columns were subsequently washed with distilled water and recharged with Cu(II) ions as described.

After completion of the chromatographic separation, the appropriate peak fractions were collected and concentrated on a YM 10 membrane filter or by using Centricon 10 microconcentrators. They were then re-equilibrated in deionized water using PD-10 columns, and finally lyophilized before studying by analytical IEF.

Non-chromatographic equilibrium binding experiments. The experiments were performed essentially as described by Hutchens *et al.* [13] and Hutchens and Yip [19], using commercial AAG after desialylation. IDA Sepharose gel loaded with Cu(II) ions, as described in the preceding section, and equilibrated in pH 7 buffer E, was allowed to settle in a 10-ml graduated cylinder to a constant final bed volume (at least 45 min). A homogeneous gel suspension (50%, v/v) was prepared in buffer E and 100- or 200-μl aliquots (50 or 100 μl gel, respectively) were dispensed into quadruplate sets of small polyethylene incubation tubes containing 100 μl of desialylated AAG solution in buffer E, at eleven different concentrations (1–30 μM). The final 300-μl volume in the tubes was adjusted with buffer E. The tubes were incubated for 30 min at room temperature and shaken intermittently to produce adequate mixing, and then centrifuged (30 s at 1200 rpm) using a table top centrifuge to pellet the gel. A 100-μl volume of the clear supernatant was sampled from each tube for spectrophotometric determination at 278 nm of the unbound protein concentrations.

To correct the absorbance values for background absorbance, "blank" tubes containing 100 or 200 μl (depending upon the assay) of the homogeneous IDA–Cu(II) gel suspension in 300 μl (final volume) of buffer E were treated under the same conditions as those described for the binding assays. The background absorbance low values, measured in 100 μl of the supernatant from the "blank" tubes, were then subtracted from the "unbound protein" absorbance values.

Equilibrium binding assays were also performed with HSA used as a control protein. A constant volume (50 μl) of the homogeneous gel suspension (25 μl gel) was added to 100 μl of HSA solution in buffer E at eleven different concentrations (5–75 μM). Other details are identical to those described for the binding assays with desialylated AAG.

Calculations. Equilibrium concentrations of unbound (free) protein ([P]) in the supernatant were subtracted from the total protein added to determine ligand-bound protein ([PL]) at each concentration. The data were plotted on a Scatchard plot [20].

To calculate the apparent affinity constants of desialylated AAG and HSA for immobilized Cu(II) ions, the experimental values were fitted according to non-linear regression analysis, using the MICROPHARM program [21] on a Tandon IBM PC. This program was developed at the Institut National de la Santé et de la Recherche Médicale (INSERM, Paris, France) and estimates parameters with their standard deviations using an iterative Gauss–Newton algorithm. For statistical analysis, the *F*-test was applied to determine the best fit. One-class and a two-class binding-sites models were used to adequately fit the experimental results obtained with desialylated AAG and HSA, respectively.

RESULTS

Purification of AAG from individual plasma samples on immobilized Cibacron Blue F3G-A

The three main AAG phenotypes samples (F1S/A, F1/A and S/A AAG) were separately purified by chromatographic separation of individual human plasma samples on Cibacron Blue F3G-A immobilized to Sephadex G-100, in 10 m*M* sodium phosphate buffer pH 5.8, essentially as described by Hervé *et al.* [10]. Beforehand, ali-

quots of the human plasma samples used in the chromatographic procedure were desialylated with neuraminidase and the AAG phenotype was then determined (results not shown). The relative proportions of each variant in the desialylated whole plasma used, as found by scanning, are given in Table I.

After completion of chromatography, the only constituent detected in the breakthrough fraction was AAG, as a single protein band was found by SDS-PAGE (Fig. 1). The calculated M_r (44 kilodaltons) was identical with that of commercial AAG. The purity and the identification of AAG in the chromatographic fractions were also confirmed by immunoelectrophoresis on agarose gels (results not shown), as a single arc-like immunoprecipitate was obtained using a specific antiserum to human plasma proteins and anti-human AAG immunoglobulins as antibodies, respectively. On average, the chromatography of the plasma yielded 5–8 mg of AAG of each phenotype from an initial total amount of 7–10 mg AAG in each individual plasma fraction used (20 ml). The recoveries were in good agreement with those reported previously [10].

After delipidation and desialylation with neuraminidase, the microheterogeneity of the purified AAG samples was checked by analytical IEF on an immobilized pH 4.4–5.4 polyacrylamide gel gradient under denaturing conditions [with 8 *M* urea and 2% (v/v) 2-mercaptoethanol]. The desialylated AAG samples were found to contain either the three main genetic variants (F1S/A AAG) or the "fast" F1 and the "slow" A variants (F1/A AAG) or both the "slow" S and A variants (S/A AAG), respectively (Fig. 2). These results agreed with the AAG phenotyping of the plasma used. Several faint, more anodic bands were also observed after staining with Coomassie Brilliant Blue (Fig. 2), indicating the presence of a small proportion (less than 5%) of incompletely desialylated protein. The relative proportions of each variant in the desialylated AAG samples, as found by scanning, are given in Table I and the values are in accordance with the relative proportions of the variants in desialylated whole plasma.

TABLE I

APPROXIMATE p*I* VALUES OF THE AAG VARIANTS AND THEIR RELATIVE PROPORTIONS IN THE INDIVIDUAL DESIALYLATED WHOLE PLASMA SAMPLES AND IN THE PURIFIED AAG SAMPLES AFTER DESIALYLATION

Phenotype	F1 variant			S variant			A variant		
	Relative percentage		p*I*[c]	Relative percentage		p*I*[c]	Relative percentage		p*I*[c]
	In plasma[a]	In AAG sample[b]		In plasma[a]	In AAG sample[b]		In plasma[a]	In AAG sample[b]	
F1S/A	33	32	4.7	34	36	4.8	33	32	4.8
F1/A	49	52	4.8	–	–	–	51	48	4.9
S/A	–	–	–	60	62	4.8	40	38	4.8
Commercial AAG	–	41[d]	–	–	31[d]	–	–	28[d]	–

[a] Relative proportions of the variants in the desialylated individual whole plasma samples were determined by scanning after IEF of the sera in an immobilized pH 4.4–5.4 polyacrylamide gel gradient with 8 *M* urea and 2% (v/v) 2-mercaptoethanol and detection by immunoblotting with two antibody steps.

[b] Relative proportions of the variants in the desialylated AAG samples were those determined by scanning the gel shown in Fig. 2.

[c] p*I* values were determined from the patterns shown in Fig. 3 and correspond to the point of the pH gradient at which each mobility line crossed over the application trench.

[d] Relative proportions of the variants in the desialylated commercial AAG sample were those determined by scanning the gel shown in Fig. 6 (lanes 1 and 10).

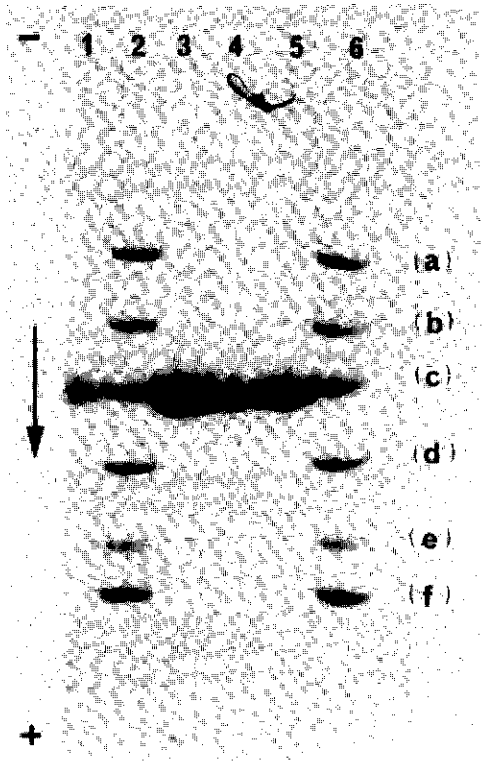

Fig. 1. SDS-PAGE of the AAG samples separately purified by chromatography of individual human plasma sample on immobilized Cibacron Blue F3G-A. Lane 1, standard commercial human AAG (≈5 μg); lanes 2 and 6, molecular mass markers, (a) phosphorylase b (94 kilodaltons), (b) albumin (67 kilodaltons), (c) ovalbumin (43 kilodaltons), (d) carbonic anhydrase (30 kilodaltons), (e) trypsin inhibitor (20 kilodalton), (f) α-lactalbumin (14 kilodaltons); lanes 3, 4 and 5, purified S/A, F1S/A and F1/A AAG samples (≈7.5 μg). Staining of the proteins was carried out with Coomassie Brilliant Blue R-250.

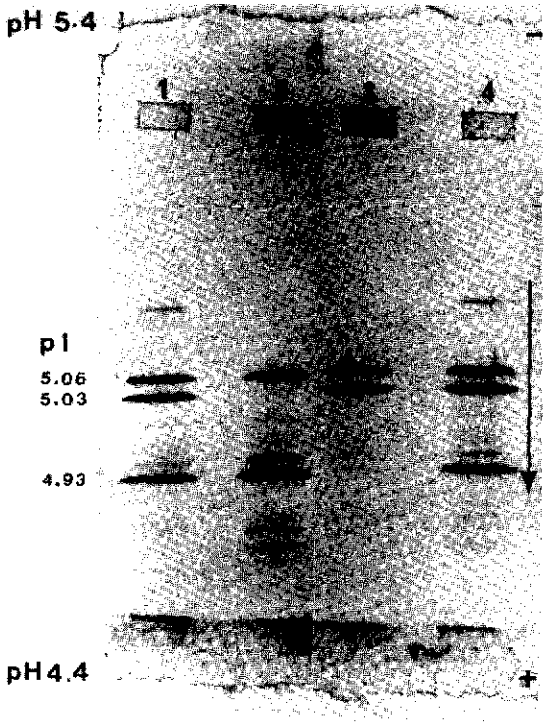

Fig. 2. IEF on immobilized pH 4.4–5.4 polyacrylamide gel (4.85%, w/v) gradient with 8 *M* urea and 2% (v/v) 2-mercaptoethanol of the purified AAG samples after desialylation with neuraminidase. Desialylated AAG samples (25 μg) with the F1S/A (lanes 1 and 4), F1/A (lane 2) and S/A phenotype (lane 3). Detection of the desialylated variants in the gel was carried out by staining with Coomassie Brilliant Blue R-250. The pH scale and the approximate isoionic point (p*I*) value for each variant are indicated.

pH titration curves of the desialylated variants of human AAG

The pH titration curves of the desialylated AAG samples with different phenotypes were obtained by running the proteins, under non-denaturing conditions, in two different pH gradients (within the pH ranges 3.5–9.5 and 5–8, respectively), using a two-dimensional IEF–electrophoresis technique [11].

Fig. 3a–3c shows the curves obtained by running the proteins in a pH 3.5–9.5 gradient. When electrophoresis was performed perpendicularly to the pH gradient, the desialylated AAGs moved in the gel according to their titration curves. At each level along the migration path the proteins picked up or released protons, as a function of the prevailing pH of the medium, according to the pK_a values of their ionizable groups. As AAG was run in the desialylated state, only the surface amino acid charged groups, directly accessible to the solvent, were expected to become titrated and to contribute to the glycoprotein net charge and electrophoretic migration.

Depending on the phenotype, the titration curves showed one or two major mobility lines. The point of the pH gradient at which each line crossed over the application trench corresponded to the p*I* value of the protein which, at this level, had no net charge and stopped migrating. The curves of F1S/A (Fig. 3a) and F1/A AAG (Fig.

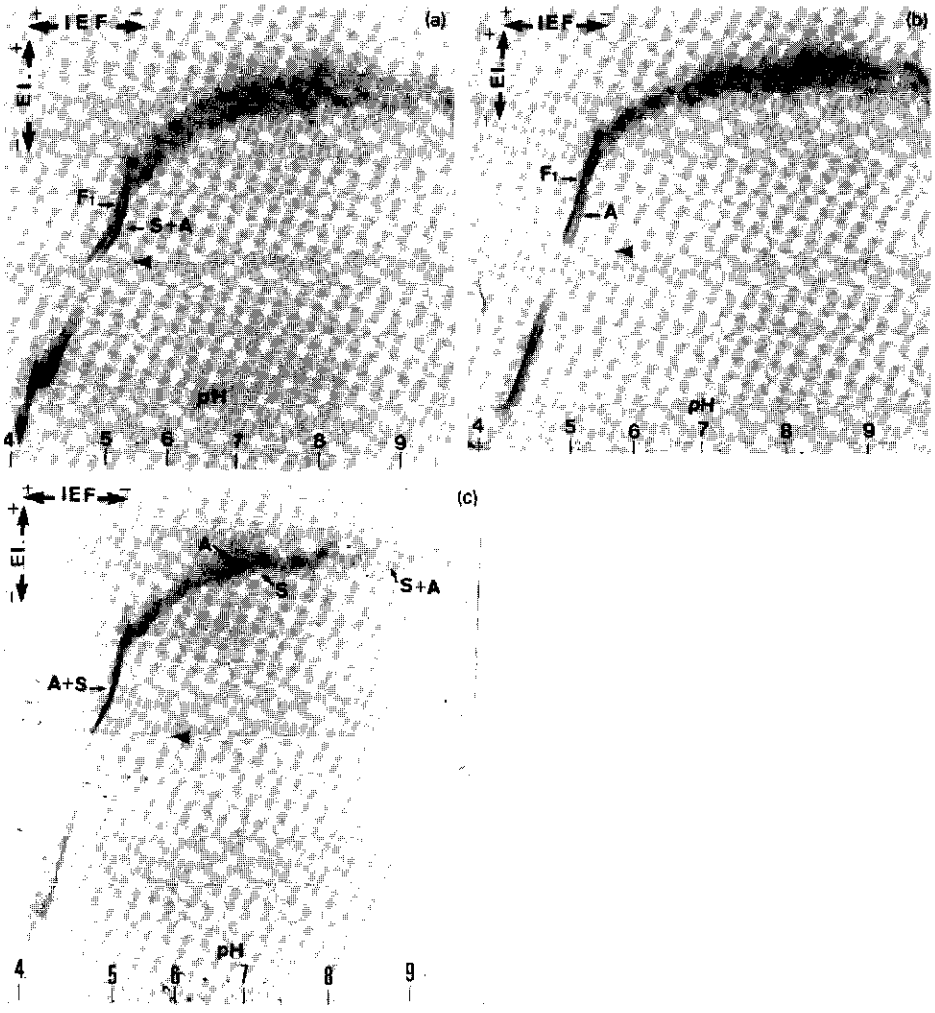

Fig. 3. Titration curves of (a) the desialylated F1S/A, (b) F1/A and (c) S/A AAG in a pH 3.5–9.5 gradient gel. The two double arrows and positive and negative symbols represent the direction and polarity of IEF and electrophoresis. The point of the pH gradient where each mobility line crosses the sample slot (indicated by an arrowhead) indicates the isoionic point (p*I*) of each variant species. Gel slab (10.9 × 11.4 × 0.2 cm): 5% T, 3% C_{bis} and 2.4% Ampholines pH 3.5–9.5. First dimension (IEF): 90 min run in the LKB 2117 Multiphor Chamber by delivering 10 W (constant); coolant temperature, 4°C. Second dimension (electrophoresis): 25 min run at 700 V (constant) with a sample load of approximately 100 μg of each variant species in deionized water. Staining: 0.115 g% (w/v) Coomassie Brilliant Blue R-250 in 25% (v/v) ethanol and 8% (v/v) acetic acid. Magnification factor of 1.11. The faint protein band which was observed above the S and A variants mobility lines in Fig. 3c probably contains a small proportion of incompletely desialylated S/A AAG. In addition, the apparent increase and decrease in mobility at the acidic and alkaline end of the titration curves, respectively, were artefacts, probably due to an edge effect or to interactions of the proteins with carrier ampholytes, or both.

3b) both showed one upper and one lower mobility line which were crossing over the application trench at values which were about 4.7 and 4.8 pH units, respectively. In addition, for S/A AAG (Fig. 3c), only one mobility line crossed over the application trench at a pH value of about 4.8, confirming that the S and A variants have the same p*I* value when they are run under non-denaturing conditions [7]. Referring to the p*I* values (Table I), it was inferred that the upper mobility line could be identified as the F1 variant in the titration curves of F1S/A and F1/A AAG, whereas the lower line in the curve of F1/A AAG was due to the A variant. In addition, the lower mo-

bility line in the titration curve of F1S/A AAG, as well as the nearly single line in the curve of S/A AAG, consisted of variants S plus A.

The pH–mobility profiles shown in Fig. 3a–c indicated that all the AAG variants moved almost together along the major part of the pH 3.5–9.5 gradient, following a hyperbolic path. As the pH was gradually increased from about 3.5 to 5.5, the proteins followed an almost straight path and crossed steeply over the application trench. Owing to the steepness of the titration curves in this pH zone, it seemed that numerous protons were then lost or acquired by the AAG variants. Indeed, the desialylated variants acquired their maximum negative net charge only about 0.5 pH units above the p*I* plane. Moreover, the nearly straight section on the acidic side of the titration curves seems to indicate that modifications in the net charge of the variants were constant between about pH 3.5 and 5.5.

Modifications in the protein net charge along the acidic branch of the titration curves are expected to be due to the gradual (de)protonation of the dissociating acidic groups. From the results obtained it may be therefore hypothesized that numerous acidic residues were exposed at the surface of the desialylated variants and, further, that the side-chain charged groups of these residues had relatively close range of pK_a values [22]. This working hypothesis needs to be confirmed by chemical evidence. Nevertheless, it appears to be in agreement with the acidic p*I* values of the AAG variants and to be supported by the previous results of Schmid *et al.* [23], who showed that, on specific chemical modification, 18 of the 26 amino acid carboxylic groups of human AAG are rapidly amidated (*i.e.* are free and accessible), when the protein is in the "native" configuration.

In the pH zone of about 5.5–7.5, the pH–mobility curves of the AAG variants showed a smoothly curved shape. However, depending on the AAG phenotype, the differences in total charge between the variants were found to become minimal or maximal along the neutral zone of the pH gradient, as the ionizable groups involved were gradually titrated in this pH zone. In the F1/A AAG titration curve (Fig. 3b), the A and F1 variants, which moved as two parallel and different fronts between about pH 3.5 and 5.5, seemed to migrate closer and to mix as the pH was progressively increased from about 5.5 to 7.5, indicating that the charge differences between the two species became minimal at this point. In contrast, in the curve of S/A AAG (Fig. 3c) the S and A variants, which formed a single front between about pH 3.5 and 5.5, moved as two close, but different mobility lines between about pH 5.5 and 7.5, indicating that the slow variants showed significant differences in total charge only along the neutral zone of the pH gradient.

The detection of the variants in the neutral pH zone was further optimized by running the S/A and F1S/A AAG samples in a pH 5–8 gel gradient. These titration curves are shown in Fig. 4a and b, respectively. The curve obtained by running the S/A AAG sample confirmed that the S and A variants moved as two close but still different fronts between about pH 6.5 and 7.5. The upper line was identified as the A variant and the lower line as the S variant, given the relative proportions of the two species in the S/A AAG sample (Table I). In addition, when the F1S/A AAG sample was run in a pH 5–8 gradient, the A variant could be individually detected along about the pH zone 6.5–7.5 as a very thin mobility line running exactly between the upper and lower lines of variants F1 and S, respectively. However, from neutral to alkaline pH values, the titration curves of S/A and F1S/A AAG (Fig. 4a and b) showed that the mobility lines of variants A and S converged and met at around pH 7.5. Then, at pH values higher than about 7.5, the two variants moved in the gel as a single front. This was also observed when the titration curve of S/A AAG was displayed in a pH 3.5–9.5 gradient (Fig. 3c). These results seemed to indicate that, after complete titration of the ionizable groups involved in the neutral zone of the pH gradients, variants S and A did not show detectable differences in total charge. Moreover, when F1/A AAG was run in a pH 3.5–9.5 gradient (Fig. 3b), variants F1 and A, which seemed to mix between about pH 5.5 and 7.5, were found to move apart at pH values high-

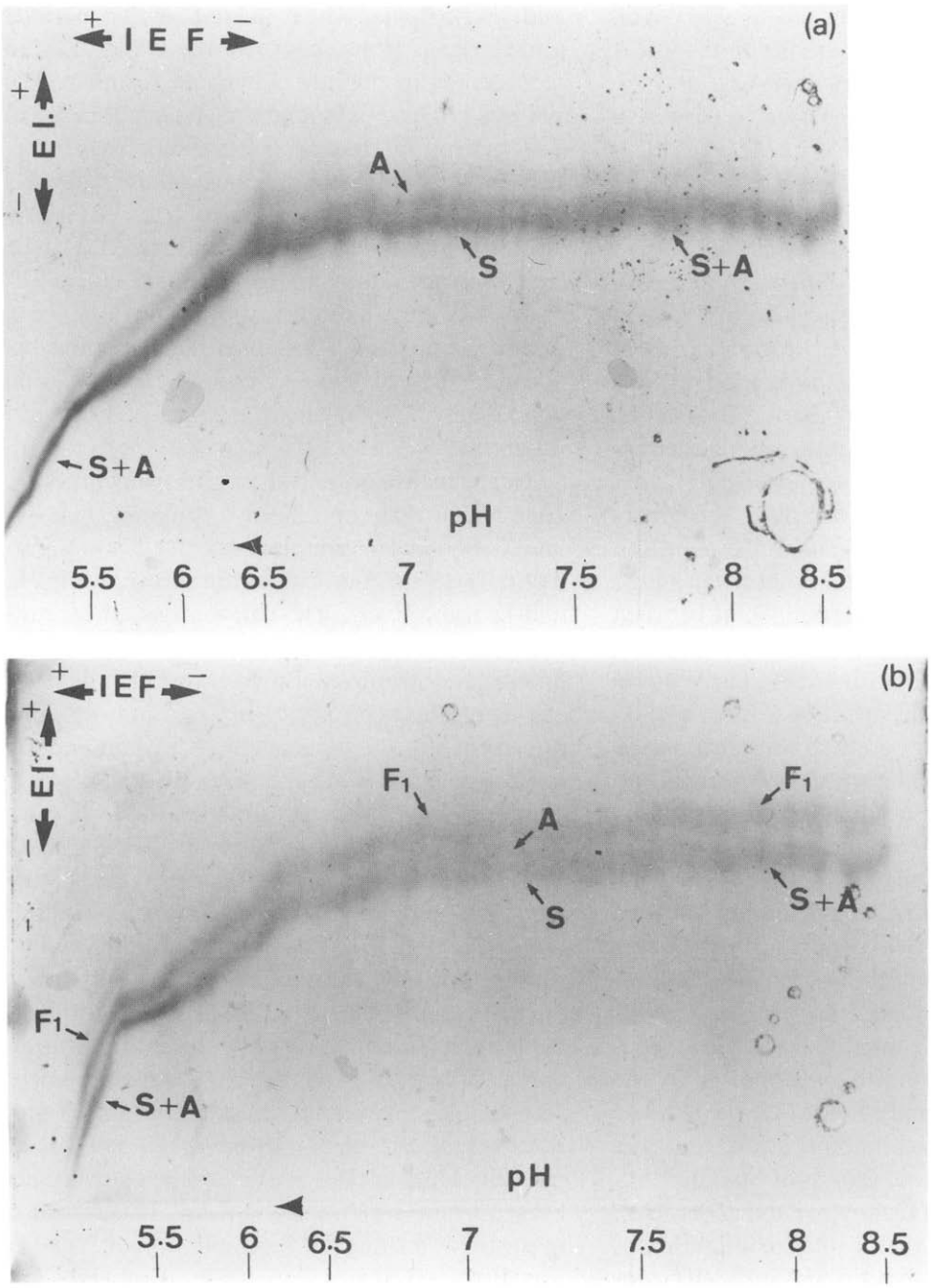

Fig. 4. Titration curves of the desialylated (a) SIA and (b) FIS/A AAG in a pH 5–8 gel gradient. First dimension (IEF): 75 min at 10 W (constant). Second dimension (electrophoresis): 25 min at 700 V (constant); coolant temperature, 4°C. All other details as in Fig. 3. Magnification factor of 1.3. The faint anodically migrating protein band observed in (a) is probably due to a small proportion of incompletely desialylated AAG.

er than about 7.5. Then, in the alkaline zone of the pH 3.5–9.5 gradient, the two variants moved as two distinct lines. However, as variants F1 and A were nearly the same distance apart in the acidic (below about pH 5) and in the alkaline (above about pH 8) regions of the pH gradient, the results seemed to indicate that the two variants nearly showed the same differences in total charge before and after complete titration of the radicals involved in about pH zone 5.5–7.5.

Finally, from about pH 7.5 to the alkaline end of the pH gradient (Fig. 3), a constant mobility was apparently achieved for all the AAG variants, which behaved as flat bands which were parallel to the application trench, indicating that no significant charge modifications occurred in the proteins along this pH zone.

Interactions of the desialylated AAG variants with immobilized Cu(II) ions

Interestingly, the AAG variants were found to show microheterogeneity in their total charge along the neutral branch of the pH titration curves. Given the neutral values in this region of the pH gradient, we assumed that the microheterogeneity was due to the existence of differences between the titratable histidyl residues of the AAG variants.

Transition metal ions, either in the free form in solution [24] or immobilized [12], are known to interact with specific predetermined protein surface-accessible residues. Among them, the histidyl residues are well identified metal chelate forming residues [25]. Therefore the possibility that AAG variants might interact differently with immobilized affinity metal adsorbents was investigated using an analytical chromatographic method.

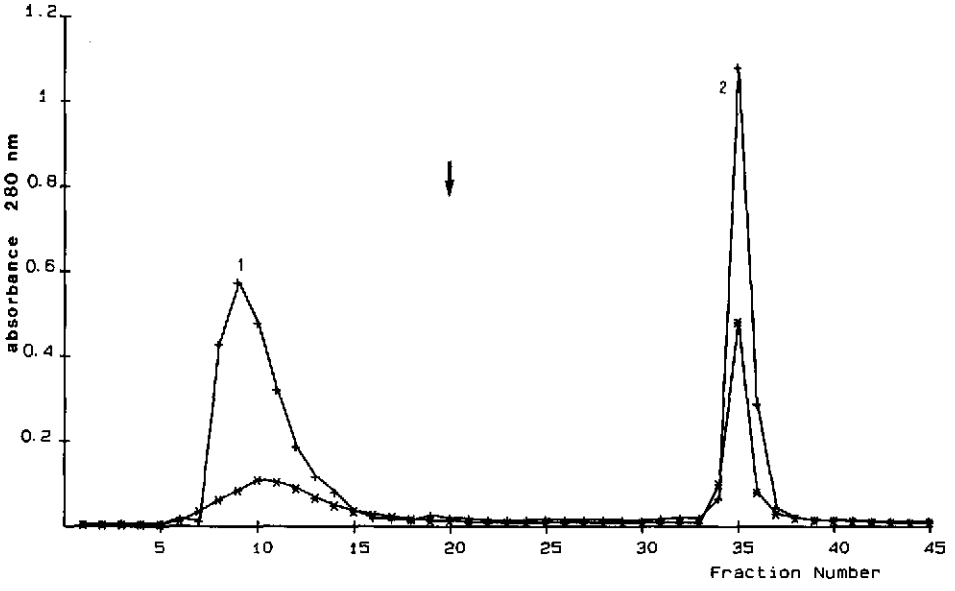

Fig. 5. Elution of the AAG variants by affinity chromatography of desialylated AAG samples on IDA–Cu(II) gel at pH 7. The affinity gel was packed into small glass columns (0.7 cm I.D.) to a final bed volume of 7.5 ml. Commercial AAG (+), or individually purified AAG samples with the F1/A or S/A (*) phenotype, were dissolved in column equilibration buffer E (5 and 1.5 mg in 0.5 ml, respectively) and applied to the columns equilibrated with the same buffer at room temperature (20 to 23°C). The flow-rate was 7.5 ml/h and fractions of 1.5 ml were collected. The absorbance of each fraction was determined spectrophotometrically at 280 nm. After several volumes of pH 7 column equilibration buffer E had been applied to remove unbound protein(s), 20 m*M* imidazole was introduced (indicated by an arrow) to elute high-affinity protein(s). The total protein recovery exceeded 90% in all experiments. Desialylated AAG peaks 1 and 2 were pooled separately, concentrated, then re-equilibrated in deionized water and finally lyophilized. To be characterized, both peaks were then subjected to analytical IEF.

Affinity chromatography on immobilized Cu(II) ions

Affinity chromatography was performed using Cu(II) ions immobilized to an IDA Sepharose [IDA–Cu(II) gel]. The experiments were carried out at room temperature (20–23°C) in pH 7 equilibration buffer E, as described under Experimental. The AAG samples used in the chromatographic experiments, after previous desialylation, were from commercial source, *i.e.* a mixture of the F1, S and A variants with respective proportions as given in Table I, and also from individually purified AAG samples with either the F1/A or S/A phenotype. Fig. 5 illustrates the elution profiles obtained by affinity chromatography of the different desialylated AAG samples with small columns of IDA–Cu(II) gel (bed volume 7.5 ml) equilibrated at pH 7. The elution diagrams show that only one protein peak (peak 1) was observed to elute with several volumes of the pH 7 column equilibration buffer E, irrespective of the origin of the desialylated AAG sample used. The introduction of 20 m*M* imidazole in buffer E to elute high-affinity proteins was followed by the elution of a second peak of desialylated AAG (peak 2). The elution volumes measured for the "unbound" (peak 1) and "bound" (peak 2) fractions of desialylated AAG, respectively, were very similar in the various chromatographic experiments, thus indicating that these volumes did not vary significantly with the variant composition of the desialylated AAG samples.

The total recovery of desialylated AAG, which was measured in peaks 1 and 2, exceeded 90% in all chromatographic experiments. However, integration showed that peak 1 consisted of about 68, 50 and 60%, and peak 2 about 32, 50 and 40% of the commercial AAG, F1/A and S/A samples, respectively.

Each chromatographic peak was concentrated with an Amicon YM 10 membrane filter or using Centricon 10 microconcentrators, then re-equilibrated in deionized water on PD-10 Sephadex G-25 columns and finally lyophilized.

Peaks 1 and 2 isolated from the different chromatographic experiments were characterized by analytical IEF in an immobilized pH 4.4–5.4 polyacrylamide gel gradient with 8 *M* urea and 2% (v/v) 2-mercaptoethanol, and the electrophoretic patterns are shown in Fig. 6. Depending on the desialylated AAG sample used in the chromatography, peak 1 was found to consist of a mixture of the F1 and S variants (commercial AAG sample) or to migrate with the F1 (F1/A AAG sample), or the S (S/A AAG sample) variant. However, for all AAG samples, peak 2 was found essentially to contain the A variant.

Therefore it was concluded from these results that the A variant was the fraction of desialylated AAG strongly bound to IDA–Cu(II) gel, and that the F1 or S variants, or both, were the unbound fraction of the protein, thus appearing to show no significant binding affinity for immobilized Cu(II) ions.

The chromatographic recoveries in the variants, as calculated by integration of peaks 1 and 2 (see earlier), were in good agreement with the proportion of each variant in the F1/A, S/A and commercial AAG samples (see Table I), respectively.

Non-chromatographic equilibrium binding experiments

The affinity chromatographic results were further supported by the equilibrium binding study of desialylated AAG to immobilized Cu(II) ions. The binding experiments were performed using a non-chromatographic protocol, previously described and validated by Hutchens *et al.* [13], which allows the rapid determination of quantitative relationships of immobilized metal affinity adsorbents for proteins. As relatively large amounts of desialylated AAG were used in the non-chromatographic binding experiments, these were performed using only commercial AAG after desialylation.

In the measurement of high-affinity immobilized Cu(II) protein interactions, Hutchens and Yip [19] have previously shown that, in the presence of buffers with a background absorbance at 278 nm (uncorrected), the "unbound protein" (*i.e.* absorbance) can be artificially overestimated in the region where there is little unbound protein

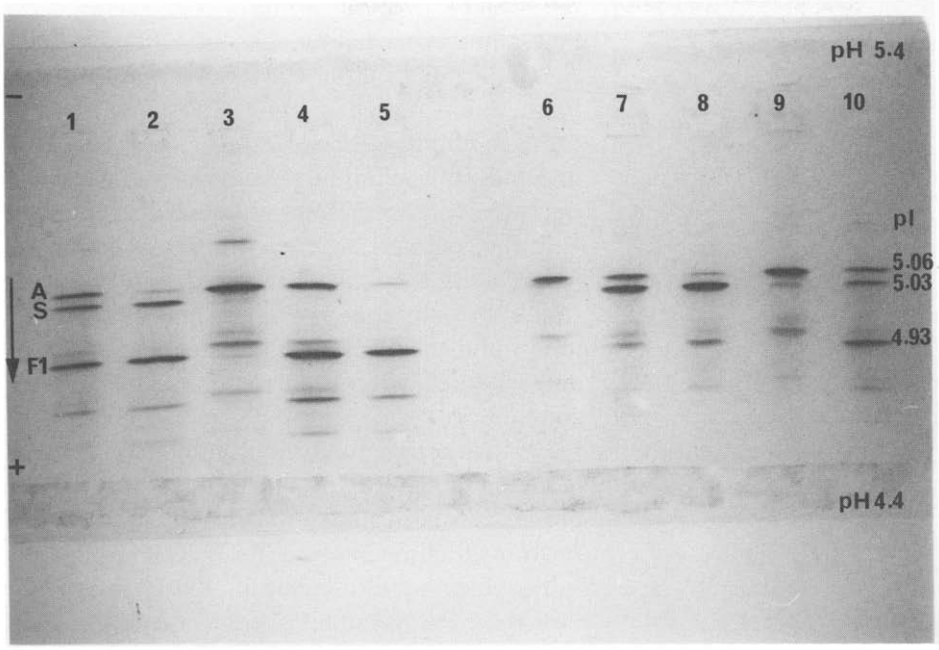

Fig. 6. Electrophoretic patterns on immobilized pH 4.4–5.4 polyacrylamide (4.85%, w/v) gel gradient with 8 *M* urea and 2% (v/v) 2-mercaptoethanol, of the isolated peaks 1 and 2, after affinity chromatography on IDA–Cu(II) gel of different desialylated AAG samples. Tracks: 1 and 10 = commercial AAG after desialylation (20 μg); 2 = peak 1 (variants F1 and S, 20 μg) and 3 = peak 2 (variant A, 20 μg), fractionated by affinity chromatography from desialylated AAG of commercial source; 4 = desialylated F1/A AAG (20 μg); 5 = peak 1 (variant F1, 20 μg) and 6 = peak 2 (variant A, 20 μg), fractionated by affinity chromatography from desialylated F1/A AAG; 7 = desialylated S/A AAG (20 μg); 8 = peak 1 (variant S, 20 μg) and 9 = peak 2 (variant A, 20 μg), fractionated by affinity chromatography from desialylated S/A AAG. Detection of the desialylated variants in the gel was carried out by staining with Coomassie Brilliant Blue R-250. The pH scale and the approximate isoionic point (p*I*) value for each variant are indicated. Peak 1 was found to contain a very small proportion of variant A, which was always less than 3% as found by scanning (lanes 2, 5 and 8). The more cathodic and anodic protein bands, different from the A variant, which were also observed after staining with Coomassie Brilliant Blue R-250 (lanes 3, 6 and 9) did not seem to be genetic products but intense minor protein contaminants. The relative proportions of these contaminants were 15% in peak 2 fractionated from commercial AAG (lane 3), whereas they were less than 5 and 10% in peaks 2 fractionated from F1/A (lane 6) and S/A AAG (lane 9) samples, respectively.

at equilibrium. To alleviate this problem, the absorbance values measured for the "unbound protein" were systematically corrected for low values of background absorbance, as described under Experimental.

The data obtained from equilibrium binding analyses of desialylated AAG interactions with IDA–Cu(II) ions, at pH 7, were plotted according to the equations outlined by Scatchard [20]. The Scatchard plots (1 and 2) shown in Fig. 7A are representative (n = 43 and 46, respectively) of desialylated AAG and were obtained in 300 μl of total reaction volumes, with two different IDA–Cu(II) gel concentrations (50 and 100 μl; curves 1 and 2 in Fig. 7A, respectively). The Scatchard plots showed that desialylated AAG had a high affinity for immobilized Cu(II) ions. The model with one class of high-affinity binding sites, plus non-specific binding (NSB), was shown to be the most adequate and the results were independent of the ratio of desialylated AAG to gel concentrations (curves 1 and 2 in Fig. 7A).

The apparent association constant (K_a) of desialylated AAG for immobilized Cu(II) ions and the maximum IDA–Cu(II) gel protein-binding capacity were calculated for each affinity gel concentration and the values obtained are given in Table II. Only non-significant differences were observed between the K_a values and between the gel protein-binding capacities, as a function of

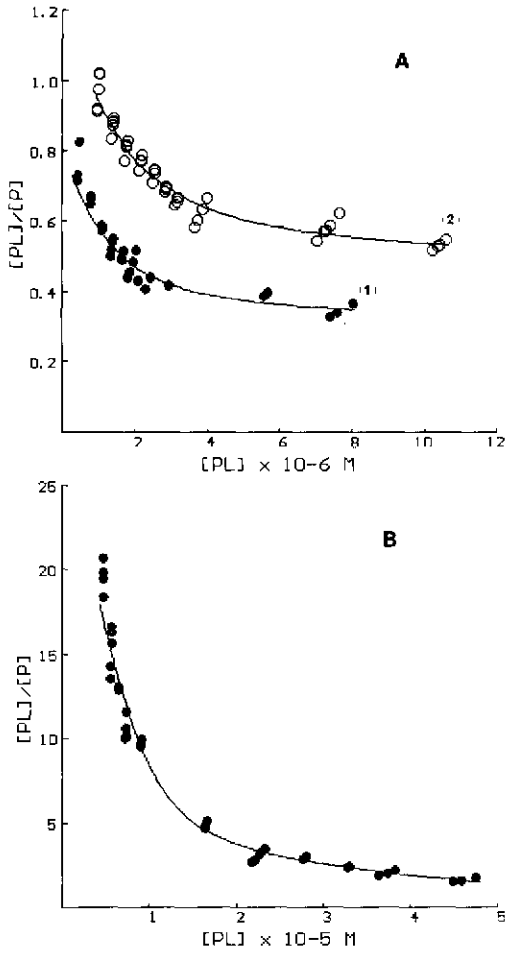

Fig. 7. Scatchard plots of equilibrium binding analyses for the interactions of desialylated AAG and HSA for immobilized Cu(II) ions. Depending on the assay, 50 or 100 μl of IDA–Cu(II) gel were allowed to interact (30 min at 23°C) with various protein concentrations in a 300-μl total reaction volume. The reaction buffer was 20 m*M* sodium phosphate (pH 7.0) containing 0.5 *M* NaCl (buffer E). The equilibrium concentrations of unbound protein, [P], were subtracted from total protein added to determine the immobilized ligand-bound protein concentrations, [PL], as described under Experimental. (A) Plots obtained for the interaction of desialylated AAG (1–30 μ*M*) with IDA–Cu(II) at two different gel concentrations (50 μl, curve 1; 100 μl, curve 2). The curves were analysed by non-linear regression with a one-class binding site model plus NSB. (B) Plot obtained for the interaction of HSA (5–75 μ*M*) with IDA–Cu(II) (25 μl). The curve was analysed by non-linear regression with a two-class binding site model. The calculated values of the apparent equilibrium association constants (K_a) and maximum IDA–Cu(II) protein-binding capacities are given in Table II.

the affinity gel concentration. On average, the high-affinity association constant of desialylated AAG for immobilized Cu(II) ions was $5.2 \cdot 10^5$ l/mol. Non-specific binding (calculated) values for each affinity gel concentration are also given in Table II. The binding results agreed well with the affinity chromatographic results obtained with the commercial AAG sample. The high-affinity binding could be ascribed to variant A, which was strongly bound by the affinity columns, and the NSB could be attributed to variants F1 and S, which were not bound by the same columns.

Furthermore, equilibrium binding control experiments were performed using HSA, as this protein has been shown to exhibit a high affinity for transition metal ions [26,27]. The binding results, which were obtained in 300-μl total reaction volumes containing 25 μl of the affinity gel, are depicted in the Scatchard plot (n = 42) shown in Fig. 7B. This plot shows that HSA strongly interacts with immobilized Cu(II) ions. However, due to its curvilinearity, the plot also suggests that HSA may be interacting non-independently or through multiple non-identical IDA–Cu(II) interaction sites. Considering the latter point, the analysis of the experimental data showed that the best fit was obtained using a two-class binding site model, with high and low affinity sites. The calculated values of the apparent association constants of HSA for immobilized Cu(II) ions, as well as the maximum IDA–Cu(II) gel protein-binding capacities, are given in Table II. In general, the binding results obtained with HSA were in good agreement with previous reports on the binding of HSA to (immobilized) transition metal ions [19,26,27].

DISCUSSION

The first objective of this investigation was to verify that the desialylated AAG variants showed charge differences in the surface titratable groups by means of a two-dimensional IEF–electrophoresis method. For this purpose, it appeared more appropriate to carry out the titration experiments, using individually purified AAG samples

TABLE II

APPARENT ASSOCIATION CONSTANTS OF DESIALYLATED AAG AND HUMAN SERUM ALBUMIN FOR IMMOBILIZED Cu(II) IONS AND IDA-Cu(II) GEL PROTEIN-BINDING CAPACITIES

k_1 and k_2 are the apparent intrinsic association constants of the high- and low-affinity sites, respectively. NSB is non-specific binding and L_1 and L_2 are the gel-binding capacities (amount of protein bound per ml of gel).

	Gel concentration					
	25 μl		50 μl		100 μl	
	Mean	S.D.	Mean	S.D.	Mean	S.D.
Desialylated AAG						
k (l/mol)	–	–	$4.81 \cdot 10^5$	2.05	$5.59 \cdot 10^5$	2.02
L [nmol protein bound/ml IDA–Cu(II) gel]	–	–	6.24	1.38	4.03	0.70
NSB	–	–	0.31	0.01	0.47	0.01
Human serum albumin						
k_1 (l/mol)	$2.81 \cdot 10^6$	1.03	–	–	–	–
L_1 [μmol protein bound/ml IDA–Cu(II) gel]	0.11	0.02	–	–	–	–
K_2 (l/mol)	$3.36 \cdot 10^4$	0.69	–	–	–	–
L_2 [μmol protein bound/ml IDA–Cu(II) gel]	0.90	0.07	–	–	–	–

with the F1/A and S/A phenotype, as they are less complex mixtures of the variants than commercial AAG samples.

Our results suggest that the titratable residues which were involved in microheterogeneity along the neutral zone of the pH gradient were the ionizable histidyl residues of the AAG variants. As a consequence, this led us to investigate the binding of the variants to immobilized Cu(II) ions using an affinity chromatographic method on IDA–Cu(II) gel. This study showed that the AAG variants exhibited heterogeneity on binding to immobilized Cu(II) ions: the A variant was strongly bound to the affinity gel, whereas the F1 or S variants, or both, were eluted in the flow-through fractions of the columns, thus indicating that these two variants had no significant binding affinity for the immobilized ligand. These results were further confirmed by equilibrium binding analyses using a non-chromatographic experimental procedure. An apparent association constant of $\approx 5.2 \cdot 10^5$ l/mol was determined for the immobilized Cu(II)–desialylated AAG interaction system, and the single class of high-affinity sites was ascribed to the A variant.

We checked whether the experimental results were related to the differences in primary structure existing between the genetic variants of human AAG. Human AAG is encoded by two different genes [5] accounting for the multiple amino acid substitutions found in its primary sequence [2,5]. Genetic studies in population at the protein level [4] have shown that variants F1 and S are encoded by two different alleles of the same gene, and would only differ by a few amino acids (possibly five). This could explain why the F1 and S variants had parallel pH–mobility curves when they were run in a pH 3.5–9.5 gradient and why the two variants had a similar behaviour on binding to immobilized Cu(II) ions. In addition, variant A is encoded by the other gene and differs from the other two variants by at least 22 amino acids. Therefore, the peculiar mobility of variant A in the neutral zone of the pH 3.5–9.5 gradient, as well as its high-affinity binding to immobilized Cu(II) ions, seem to agree with the important differences in primary structure between the A and F1/or S variants.

In particular, we looked for differences in cysteinyl, histidyl and tryptophanyl residues between the AAG variants, as these residues are potent metal chelate-forming residues at the sur-

face of proteins [25,28,29]. Examination of the possible amino acid substitutions described for the AAG variants [2,5] shows that the A variant contains a single cysteinyl residue (located at position 149 in the primary sequence), which appeared to be substituted by arginyl residues in the F1 and S variants [5]. However, previous results obtained in our laboratory (Hervé, unpublished results) suggest that the A variant cysteinyl residue is neither accessible nor free, owing to covalent binding, as this residue cannot be carboxymethylated after specific chemical modification with iodo[2-^{3}H]acetic acid. Moreover, this finding seems to be in agreement with the observation that, on the alkaline side of the titration curves (*i.e.* between about pH 7.5 and 9.5), variant A behaves as a flat band parallel to the application trench, indicating that no significant charge modifications occur in the A variant along the zone of the pH gradient where free and accessible cysteinyl residues are expected to become titrated. Examination of the primary sequence of human AAG shows that the protein has three histidyl and tryptophanyl residues. However, as none of these residues are involved in the substitutions described for the AAG variants [2,5], the microheterogeneity between the A and F1 or S variants on binding to immobilized Cu(II) ions cannot be accounted for by differences in the total number of histidyl and tryptophanyl residues. On the other hand, the interaction of proteins with immobilized metal ions is very complex, as the protein affinity depends on many factors such as the number, type, surface accessibility and relative distribution of metal chelate-forming groups (*i.e.* proximal electron donors) on the surface of protein [19]. Therefore, the only conclusion which may be drawn from the heterogeneous binding of the AAG variants to immobilized Cu(II) ions is that the A variant molecule seems to show a more favourable surface topography for binding to transition metal ions than the F1 and S variants.

Besides, the comparison of the results obtained from the study of the titration curves with those obtained from affinity binding to immobilized Cu (II) ions for the AAG variants was difficult. Indeed, in the case of the titration curves the differences observed between the variants could only be due to differences in their accessible charged residues (*i.e.* possibly the histidyl residues along the neutral zone of the pH gradient). However, the heterogeneity on binding to immobilized Cu(II) ions between the AAG variants could involve differences in both their surface charged or uncharged residues (histidyl and tryptophanyl residues, respectively), or both, as well as other features of the protein surface which could have a relatively positive or negative effect on the recognition of immobilized metal ions [19].

Nevertheless, the study of the pH titration curves of the AAG variants allowed us to further demonstrate the existence of high-affinity binding to immobilized Cu(II) ions for desialylated AAG and the existence of heterogenous binding properties between the variants for the immobilized ligand. Our finding that the A variant was responsible for high-affinity binding to immobilized Cu(II) ions seems of interest as it supports the previous hypothesis of Eap *et al.* [9], suggesting that the A variant was responsible for high-affinity binding of some drugs to desialylated AAG.

From these results it was possible to develop an affinity chromatographic method on immobilized Cu(II) ions which allowed the simple and rapid purification of the A variant and of a mixture of the F1 and S variants from commercial AAG, with recoveries exceeding 90%. As the A variant appears to be the most interesting with respect to drug binding [9], this purification method would greatly facilitate the study of the drug-binding properties of the A variant, which has never been performed so far. However, as it has not been possible to fractionate the mixture of the F1 and S variants by affinity chromatography on an IDA–Cu(II) gel, a preparative IEF technique previously described [7] has to be used to fractionate the two variants in a final step. Nevertheless the IMAC method described here could be used successfully to purify, in a single-step procedure, small amounts of the F1, S and A variants from individual preparations of AAG with the F1/A and S/A phenotypes, respectively.

ACKNOWLEDGEMENTS

This research was supported in part by research grants from the Ministère de la Recherche et de l'Enseignement Supérieur (MRES No. 87CO320), Institut National de la Santé et de la Recherche Médicale (C.R.E. No. 872014) and Fondation pour la Recherche Médicale.

REFERENCES

1 J. M. H. Kremer, J. Wilting and L. M. H. Janssen, *Pharmacol. Rev.*, 40 (1988) 1.
2 K. Schmid, in F. W. Putnam (Editor), *The Plasma Proteins, Structure, Function and Genetic Control*, Vol. I, Academic Press, New York, 2nd ed., 1975, p. 183.
3 M. F. A. Bierhuizen, M. De Witt, C. Govers, W. Ferwerda, C. Koeleman, O. Pos and W. Van Dijk, *Eur. J. Biochem.*, 175 (1988) 387.
4 C. B. Eap, C. Cuendet and P. Baumann, *Hum. Genet.*, 80 (1988) 183.
5 L. Dente, M. G. Pizza, A. Metspalu and R. Cortese, *EMBO J.*, 6 (1987) 2289.
6 D. Tinguely, P. Baumann, M. Conti, M. Jonzier-Perey and J. Schöpf, *Eur. J. Clin. Pharmacol.*, 27 (1985) 661.
7 C. B. Eap, C. Cuendet and P. Baumann, *Naunyn Schmiedeberg's Arch. Pharmacol.*, 337 (1988) 220.
8 C. B. Eap, C. Cuendet and P. Baumann, *J. Pharm. Pharmacol.*, 40 (1988) 767.
9 C. B. Eap, C. Cuendet and P. Baumann, *Clin. Pharmacol. Ther.*, 47 (1990) 338.
10 F. Hervé, J. C. Duché, N. Sportes and J. P. Tillement, *J. Chromatogr.*, 539 (1991) 405.
11 P. G. Righetti, in T. S. Work and R. H. Burdon (Editors), *Isoelectric Focusing: Theory, Methodology and Applications*, Elsevier, Biomedical Press, Amsterdam, 1st ed., 1983, p. 259.
12 J. Porath, J. Carlsson, I. Olsson and G. Belfrage, *Nature (London)*, 258 (1975) 598.
13 T. W. Hutchens, T. T. Yip and J. Porath, *Anal. Biochem.*, 170 (1988) 168.
14 K. Weber and H. Osborn, *J. Biol. Chem.*, 244 (1969) 4406.
15 P. Grabar and C. A. Williams, *Biochim. Biophys. Acta*, 10 (1953) 193.
16 M. A. Evenson and H. F. Deutsch, *Clin. Chim. Acta*, 89 (1978) 341.
17 C. B. Eap and P. Baumann, *Electrophoresis*, 9 (1988) 650.
18 *LKB Application Note 319*, LKB-Produkter, Bromma, 1981.
19 T. W. Hutchens and T. T. Yip, *Anal. Biochem.*, 191 (1990) 160.
20 G. Scatchard, *Ann. N.Y. Acad. Sci.*, 51 (1949) 660.
21 S. Urien, F. Brée, B. Testa and J. P. Tillement, *Biochem. J.*, 280 (1991) 277.
22 E. Gianazza, C. Gelfi and P. G. Righetti, *J. Biochem. Biophys. Methods*, 3 (1980) 65.
23 K. Schmid, L. H. Chen, J. C. Occhino, J. A. Foster and K. Sperandio, *Biochemistry*, 15 (1976) 2245.
24 F. R. N. Gurd and P. E. Wilcox, *Adv. Protein Chem.*, 11 (1956) 311.
25 E. S. Hemdan, Y. J. Zhao, E. Sulkowski and J. Porath, *Proc. Natl. Acad. Sci. U.S.A.*, 86 (1989) 1811.
26 S. L. Guthans and W. T. Morgan, *Arch. Biochem. Biophys.*, 218 (1982) 320.
27 J. D. Glennon and B. Sarkar, *Biochem. J.*, 203 (1982) 15.
28 E. Sulkowski, *Trends Biotechnol.*, 3 (1985) 1.
29 D. C. Rijken and D. Collen, *J. Biol. Chem.*, 256 (1981) 7035.